Am J Cancer Res 2026;16(4):1649-1660
www.ajcr.us /ISSN:2156-6976/ajcr0168230

Case Report

Pulmonary langerhans cell histiocytosis following resection of lung adenocarcinoma: a case report and diagnostic challenges

Yihao Liu[1,2*], Zhixuan Duan[1,2*], Minghui Liu[1,2], Hongbing Zhang[1,2], Yongwen Li[2], Min Wang[2], Haoling Zhang[3], Jun Chen[1,2], Honglin Zhao[1,2]

[1]Department of Lung Cancer Surgery, Center of Thoracic Surgery, Tianjin Medical University General Hospital, Tianjin 300052, People's Republic of China; [2]Tianjin Key Laboratory of Lung Cancer Metastasis and Tumor Microenvironment, Tianjin Lung Cancer Institute, Tianjin Medical University General Hospital, Tianjin 300052, People's Republic of China; [3]Department of Biomedical Sciences, Advanced Medical and Dental Institute, Universiti Sains Malaysia Kepala Batas 13200, Penang, Malaysia. [*]Equal contributors.

Received August 20, 2025; Accepted April 13, 2026; Epub April 25, 2026; Published April 30, 2026

Abstract: Pulmonary Langerhans cell histiocytosis (PLCH) is an uncommon myeloid disorder of the lung characterized by the accumulation of Langerhans-like cells within the pulmonary parenchyma. On imaging, it typically presents as nodular or cystic lesions and is closely associated with cigarette smoking. Although PLCH can occur in both children and adults, it is more frequently observed in younger smokers and is relatively rare in elderly individuals. In most cases, the disease follows a slow and sometimes self-limiting course, and systemic therapy is not routinely required. However, radiologic differentiation from malignant ground-glass nodules may be challenging. The development of PLCH after lung adenocarcinoma surgery is rare. Here, we report the case of a 72-year-old woman with lung adenocarcinoma. Following resection of a right lung nodule, molecular testing identified an EGFR exon 19 deletion, and icotinib was subsequently administered for contralateral ground-glass nodules. During postoperative follow-up, new lesions were detected in the rib adjacent to the surgical field as well as in the lung, raising concern for possible bone metastasis on imaging. Percutaneous biopsy with immunohistochemical analysis demonstrated positivity for CD1a, Langerin, and S-100, while lung adenocarcinoma-associated markers, including CK7, TTF-1, and Napsin A, were negative, supporting a diagnosis of PLCH. The next generation sequencing found BRAF V600E mutation in PLCH lesions. After symptomatic treatment and long-term follow-up, the lesions gradually improved and partially disappeared. Looking back on the previously reported cases, it is not common for PLCH and lung adenocarcinoma to coexist. In published reports, these two conditions generally have different driving gene changes, and their potential biological relationship is still unclear. This case shows that when new lesions are found after lung cancer surgery, besides tumor recurrence, other diagnoses, namely PLCH, should be considered, and the diagnosis should be confirmed by histopathological examination.

Keywords: Lung adenocarcinoma, pulmonary langerhans cell histiocytosis, icotinib, BRAF V600E, differential diagnosis

Introduction

Langerhans cell histiocytosis (LCH) is a rare inflammatory myeloid tumor disease, which is characterized by significant heterogeneity and involving multiple organs or systems. Lung Langerhans cell histiocytosis (PLCH) is a single systemic form of LCH confined to the lung, and the proliferation of Langerhans-like cells causes progressive damage to lung parenchyma. The incidence of PLCH is about one in a million, and its pathogenesis has not been fully understood. Smoking is the main risk factor [1]. The disease most often affects young people and middle-aged people between the ages of 20 and 40.

Pathologically, PLCH is characterized by inflammatory infiltration around bronchi, followed by destruction of lung tissue structure. Chest CT often shows multiple cystic changes, ranging from hollow nodules to thin-walled cysts [2, 3].

https://doi.org/10.62347/WCGK1409

Table 1. The patient's basic characteristics and information

Characteristics		
Age	72	
Gender	Female	
Symptoms	None	
Imaging (CT)	Right Upper Lobe (Posterior Segment)	1.2 × 0.9 cm
	Right Lower Lobe (Dorsal Segment)	0.8 × 0.5 cm
	Left Upper Lobe	0.7 × 0.5 cm & 0.9 × 0.7 cm
Smoking history	None	
Family history	None	
Pathology		
Immunohistochemistry	Lung pathology	Lung adenocarcinoma
		CK7(+), TTF-1(+), NapsinA(+), CEA(+)
		EGFR (p.L747_T751del)
Genetic mutations	Postoperative soft tissue pathology	PLCH
		CD1a(+), S-100(+), Langerin(+), Bcl-2(+), STAT6(+), Vimentin(+)
		BRAF V600E
Treatment	icotinib (125 mg three times daily)	
Status	Alive	

Multi-system LCH can involve multiple organs, the most common ones are skeletal system, lymph nodes and skin, and the central nervous system, liver and spleen are less involved.

Lung cancer is still the main cause of cancer-related morbidity and mortality worldwide, and non-small cell lung cancer accounts for 85% of all cases [4]. Low dose computed tomography (LDCT) plays an important role in early detection and screening [5]. Ground glass nodules (ggn) account for a large proportion of lung nodules detected by imaging [6]. Persistent ggn may be related to precancerous lesions or early malignant tumors, so long-term follow-up and dynamic radiological examination are needed.

Some imaging features of PLCH, such as ggn, are very similar to ggn associated with lung adenocarcinoma. When they coexist or occur one after another, it will lead to confusion in diagnosis [7]. Compared with systemic LCH, PLCH generally has an unpredictable but usually inert course, mostly confined to the lungs, with little progressive spread, and the overall prognosis is better. When extrapulmonary involvement is present, bone lesions are most common and are usually osteolytic in nature [3, 8, 9]. In contrast, most early-stage lung adenocarcinomas presenting as GGNs are managed surgically and are less likely to present with bone metastasis at diagnosis [5].

In this report, we describe a female patient who developed PLCH following surgery for lung adenocarcinoma. The radiologic characteristics, histopathological and immunohistochemical findings, and underlying molecular alterations of PLCH are discussed, with the aim of improving the differential diagnosis between PLCH and lung cancer-related GGNs.

This case report was reviewed and approved by the Ethics Committee of Tianjin Medical University General Hospital (IRB2024-YX-045-01, Supplementary Materials). Written informed consent was obtained from the patient for publication of the detailed clinical information and associated images.

Case presentation

The patient, a 72-year-old woman, was found to have multiple bilateral GGNs during a routine health screening. She was later assessed at the Department of Thoracic Surgery, Tianjin Medical University General Hospital for further evaluation. Detailed baseline information and clinical features are given in **Table 1**, and the overall diagnosis and treatment schedule is shown in **Figure 1A**. Contrast-enhanced CT of the chest revealed a 1.2 × 0.9 cm solid lesion in the posterior segment of the upper lobe of the right lung. Another smaller nodule, 0.8 × 0.5 cm in size, was located near the pleura in the dorsal segment of the right lower lobe. In

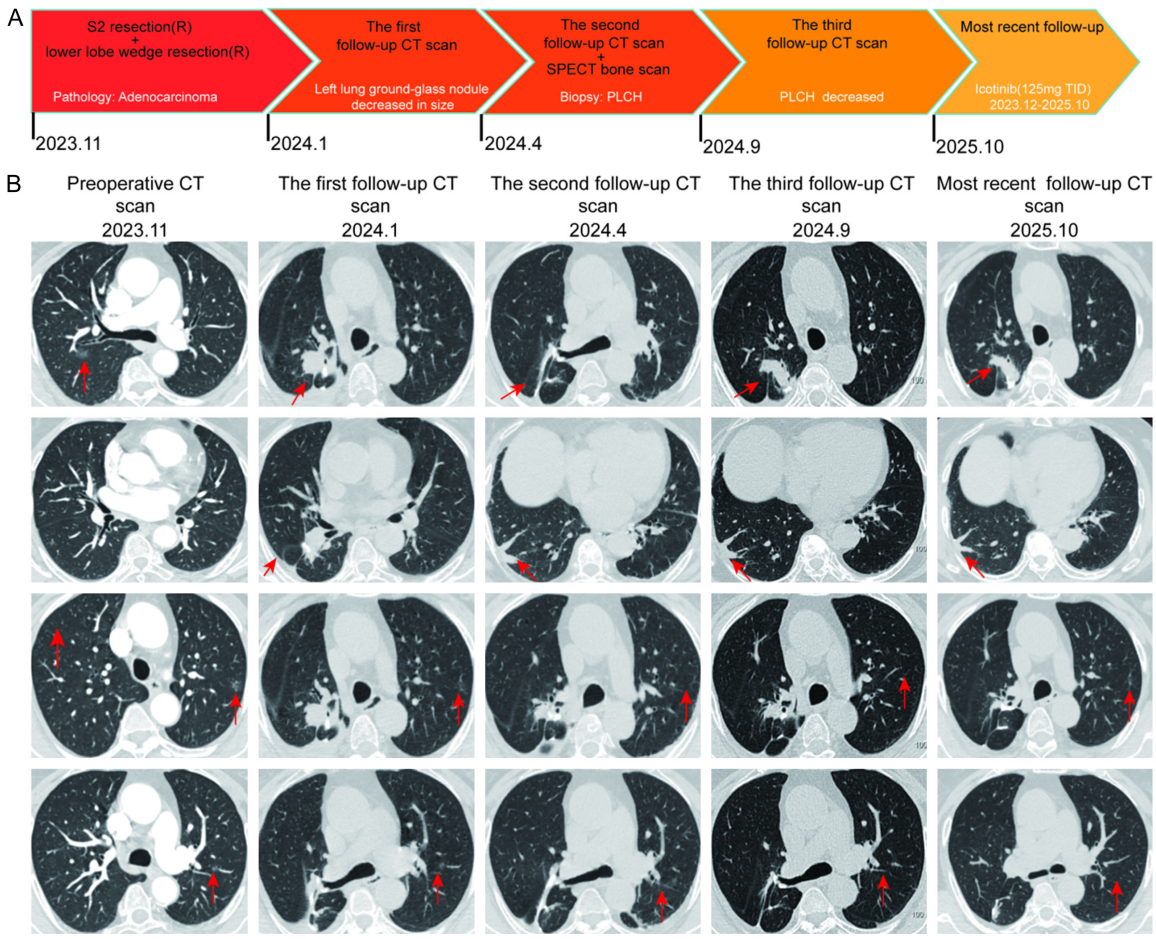

Figure 1. Diagnostic and follow-up imaging. A. The diagnostic, treatment, and follow-up steps of the patient. B. Comparison of four sequential chest CT scans.

addition, there were two sub-solid nodules in the upper lobe of the left lung, which are 0.7 × 0.5 cm and 0.9 × 0.7 cm respectively. She has a history of coronary artery stenosis, so she has been taking aspirin. Deny a history of smoking. After evaluating the indications and considering the size and number of nodules, right lung surgery was prioritized (left lung surgery is planned later). Preoperative pulmonary function testing showed preserved ventilatory function with mildly reduced diffusion capacity. The major parameters were as follows: FVC 2.63 L (95.8% predicted), FEV1 2.01 L (99.9% predicted), FEV1/FVC 76.44%, DLCO 4.83 mmol/min/kPa (76.2% predicted), and TLC 4.66 L (81.8% predicted). The surgical methods include single-port thoracoscopic right upper lobe segmental resection (S2) and right lower lobe wedge resection. Preoperative CT-guided localization of the posterior segment of the right upper lobe was performed. During surgery, both nodules were successfully removed based on localization, accompanied by lymph node dissection. The postoperative course was uneventful overall. Apart from mild cough and sputum production, no clinically significant postoperative complications were noted. No obvious air leak was observed during the first 2 postoperative days, and the chest drainage volume remained below 20 mL/day. The patient was discharged on postoperative day 3.

The patient was discharged on the third postoperative day. Pathological analysis revealed invasive adenocarcinoma in the right upper lobe and minimally invasive adenocarcinoma in the right lower lobe, without lymph node metastasis. Histopathological and immunohistochemical analyses showed that the tumor cells were positive for CK7, TTF-1, Napsin A, and CEA, while negative for P63, P40, chromogranin A (CgA), and synaptophysin (Syn). The

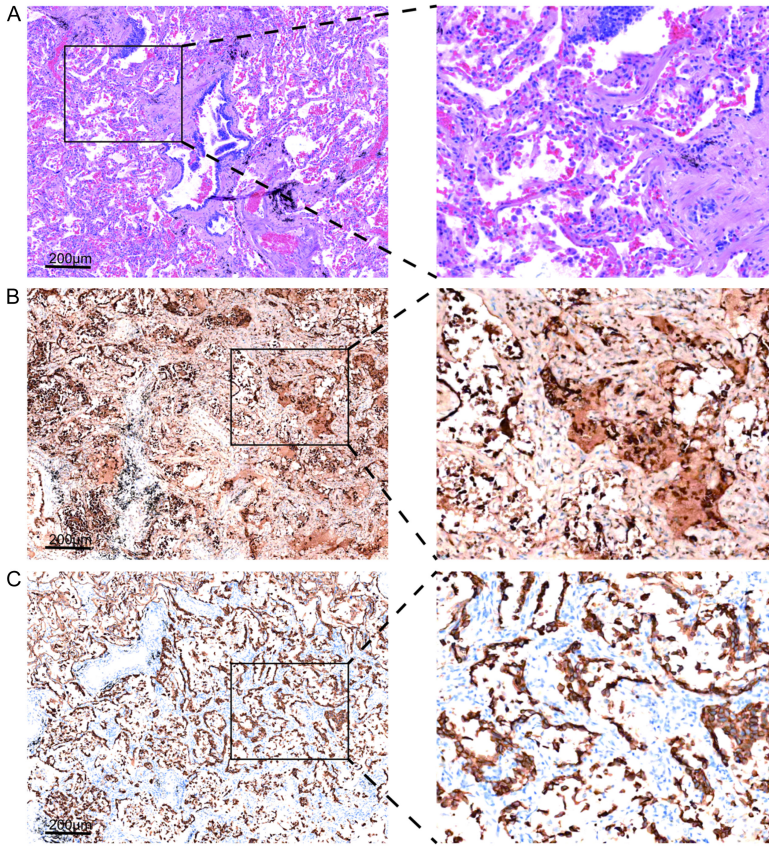

Figure 2. Pathological examination report of pulmonary nodules (10× magnification). A. Hematoxylin and eosin (H&E) staining of the pulmonary nodules. B, C. Immunohistochemical staining for CEA and CK7, respectively.

Ki-67 proliferation index was approximately 5% (**Figure 2**). Next generation sequencing (NGS) detected an EGFR mutation (c.2240_2254del, p.Leu747_Thr751del, Exon19; Geno-Truth Dx Lab). The detailed workflow and procedures for NGS are provided in Supplementary File 1. Left lung nodules were not immediately considered for surgery postoperatively. Based on Professor He's prior studies [10], oral targeted therapy can be initiated for untreated multiple primary lung nodules based on the known pathology and gene mutations of previously resected nodules. This strategy was strongly endorsed by the patient and family. Therefore, patients began to take oral icotinib (125 mg, three times a day) for targeted treatment and maintenance treatment. After two months of follow-up, the volume of GGNs in the left lung of CT became smaller and the margin was blurred. These changes are shown in **Figure 1B**.

Six months later, the patient developed persistent lower back pain due to a fall. The MRI of thoracolumbar spine showed several vertebral signal changes. At that time, these findings were interpreted as traumatic compression fractures. Subsequently, chest CT showed osteolytic lesions of the seventh rib on the right side, accompanied by thickening of soft tissue. Considering her history of lung malignant tumor, considering the possibility of tumor recurrence with rib metastasis. Compared with the early scan, the boundary of the ground-glass nodule in the left lung is unclear. Because of the uncertainty of these findings, SPECT bone scintigraphy was performed for further skeletal evaluation. The vertebral bodies at T7-T9 and L1-L3 showed superior endplate collapse and vertebral flattening, without obvious abnormal radiotracer uptake at the corresponding sites. In conjunction with the history of a recent fall, these findings were considered more consistent with compression fractures. In contrast, increased radiotracer uptake was observed at the anterior aspect of the right seventh rib, with associated bone destruction, focal cortical discontinuity, and adjacent soft tissue mass formation. The margin between the lesion and the adjacent chest wall was indistinct. Given the patient's history of lung cancer surgery, the possibility of metastatic disease could not be excluded (Supplementary Figure 1A). Because the imaging findings could not be diagnosed clearly, a biopsy of rib lesions was performed. Histological examination can support lung Langerhans cell histiocytosis. Subsequently, the next generation sequencing detected the mutation of BRAF V600E (Geno-Truth Dx Lab), and the allele frequency of mutation was 13.58%. Histopathological examination and immunohistochemical analysis of biopsy specimens showed that CD1a (20%), S-100 (20%), Langerin (10%), Bcl-2, STAT6 and vimentin were positive. CD68 and leukocyte common antigen (LCA) were partially positive. The tumor cells were negative for

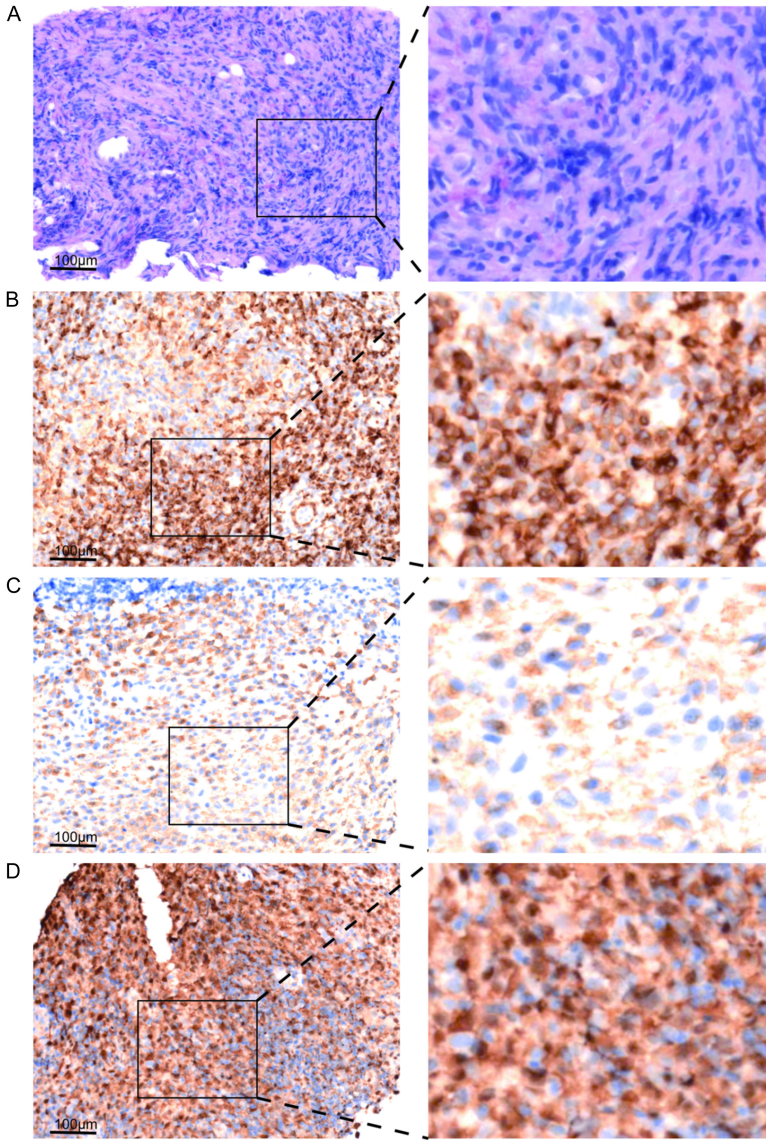

Figure 3. Pathological examination report of PLCH (20× magnification). A. Hematoxylin and eosin (H&E) staining of the PLCH lesion. B-D. Immunohistochemical staining for CD1a, Langerin, and S100, respectively.

cytokeratin (CK), CK7, thyroid transcription factor-1 (TTF-1), calretinin, and D2-40. The Ki-67 proliferation index was approximately 20% in hotspot areas (**Figure 3**). In view of the vertebral fractures and the clinical need for early functional recovery, the patient underwent bone cement augmentation. Given her lack of smoking history and the absence of intracranial involvement on routine brain magnetic resonance imaging, a strategy of close observation with regular follow-up was adopted for the pulmonary PLCH. Postoperatively, oral calcitriol and meloxicam were administered for symptomatic management, resulting in marked relief of back pain.

At the 10-month follow-up, PET/CT revealed a significant reduction in the size of the soft tissue mass adjacent to the right seventh rib. The rib showed bony destruction with sclerotic margins and increased metabolic activity (SUVmax 6.4), consistent with the imaging characteristics of Langerhans cell histiocytosis. Schmorl's nodes and chronic compression fractures were observed at T12 to L3, with mildly elevated metabolism (SUVmax 3.5), suggestive of old vertebral injuries (as seen in Supplementary Figure 1B). A 3D reconstruction model of PLCH and the affected rib is shown in Supplementary Figure 1C. Compared with previous chest CT scans, the two GGNs in the left lung had become markedly blurred or even completely resolved. During the most recent follow-up in October 2025, the patient reported that routine CT monitoring showed that the PLCH lesions had further decreased in size and remained stable, and the left-sided nodules had nearly disappeared. After bone cement augmentation, the patient was managed conservatively with rest and gradual resumption of daily activities, without formal rehabilitation training. Her back pain improved significantly after the procedure, and no procedure-related complications were reported. Because the patient had been living outside the local area for a prolonged period, subsequent follow-up was mainly performed at a local hospital. According to the available follow-up information, chest CT was performed approximately every 6 months, and the results were obtained mainly through telephone follow-up. The available reports suggested that the pulmonary and rib lesions remained overall

stable without definite evidence of progression. However, because the original imaging data and detailed records from the outside hospital were not fully accessible, a more comprehensive description of the serial follow-up findings could not be provided.

Discussion

The development of PLCH following lung adenocarcinoma resection is extremely rare, as the exact relationship between lung cancer and PLCH remains unclear. Some case studies have observed the proximity of PLCH to lung cancer tissues. Moreover, research suggests that PLCH may create a fibrotic microenvironment conducive to tumorigenesis, potentially increasing the risk of bronchogenic carcinoma, although this theory has not been definitively proven [11]. Smoking plays an important role in the development of both PLCH and lung adenocarcinoma. Cases in which the two conditions occur in the same patient are infrequent, and it remains uncertain whether one process precedes or influences the other [12]. With the more and more extensive application of chest CT in screening practice, more and more lung adenocarcinoma is detected in the early stage, which is generally manifested as GGNs [13]. Not all ggn are malignant tumors, and many are related to inflammation or other benign processes. These lesions may correspond to organizing pneumonia, granulomatous inflammation, eosinophilic pneumonia, or focal interstitial fibrosis, whereas only a subset represents adenocarcinoma or atypical adenomatous hyperplasia (AAH) [14]. GGN, which is finally proved to be malignant, generally has subtle but suggestive imaging features, namely irregular or fuzzy edges, some solid components and measurable growth over time [15]. The relatively short volume doubling time will further arouse doubts. PLCH is mostly nodules, which can form cavities or evolve into cystic lesions with uneven wall thickness. These findings can be accompanied by linear fiber bundles or scattered ground glass-like changes. Mediastinal lymphadenopathy or skeletal lesions can also be found in some patients, but they are not common. It is difficult to distinguish PLCH from lung malignant tumor on PET/CT. Both cases will show increased uptake of fluorodeoxyglucose, especially when bone is involved, which limits the specificity of metabolic imaging [3, 14, 16, 17]. It is worth noting that distinguishing bone metastases from lung cancer and osseous involvement by PLCH is highly challenging. Typical bone metastases from lung cancer usually present as moth-eaten or infiltrative osteolytic destruction with ill-defined margins and a wide zone of transition, and they generally lack a sclerotic rim. In contrast, classic osseous lesions of PLCH more often appear as well-defined “punched-out” osteolytic defects, frequently accompanied by a distinct sclerotic margin, and may show a characteristic beveled-edge appearance due to unequal destruction of the inner and outer cortical tables; a localized periosteal reaction may occasionally also be seen. However, the diagnostic pitfall is that both entities can demonstrate nonspecific hypermetabolic uptake on PET/CT. More importantly, when PLCH is in an active progressive phase, it may exhibit highly aggressive, “pseudomalignant” features, including cortical breakthrough, marked bone marrow edema, and adjacent soft tissue mass formation. Under these circumstances, PLCH can be nearly indistinguishable from metastatic malignancy on imaging alone, making timely histopathological biopsy essential for establishing the final diagnosis.

Smoking in adults is the main risk factor for PLCH, and it is also the most direct risk factor. More and more people think that the pathogenesis of PLCH is related to the abnormal activation of mitogen-activated protein kinase (MAPK) signaling pathway, most obviously through molecular changes, namely BRAF V600E mutation. Mutations will occur in hematopoietic or bone marrow precursor cells of non-smokers, which will cause clonal proliferation of abnormal Langerhans-like cells. In fact, previous studies have proved that BRAF V600E expression exists in PLCH patients who have no smoking history, which indicates that genetic changes can promote the onset of diseases independently of environmental exposure [18]. About 50-60% PLCH patients carry BRAF V600E mutation [19, 20]. This change locks the BRAF protein in the constitutively active conformation, which leads to the continuous activation of the RAS-RAF-MEK-ERK (MAPK) signaling cascade [21, 22]. Therefore, downstream effectors MEK and ERK are continuously phosphorylated, which promotes the proliferation and survival of pathological Langerhans-like cells and enhances their pro-inflammatory and tissue destruction characteristics. In addition

to brav600e, other MAP2K1 (MEK1) mutations, ARAF changes and abnormalities in MAPK-related genes, including NRAS and KRAS, were also found in the subset of PLCH cases [23]. These genetic events will trigger MAPK pathway at different signal levels, and ERK signal can be maintained even without BRAF mutation. Generally speaking, these findings indicate that the activation of constitutive MAPK pathway is the central molecular marker for the initiation and development of PLCH.

It is worth noting that this patient developed PLCH after resection of lung adenocarcinoma, which was confirmed to contain EGFR mutation by new generation sequencing, which may reflect the continuous activation of shared MAPK signal axis rather than direct molecular interaction. EGFR regulates several key downstream pathways, including RAS/RAF/MEK/ERK, PI3K/AKT and JAK/STAT, which are essential for cell survival, proliferation and immune regulation [24]. Although PLCH is considered to be a MAPK-driven clonal myeloid disease, lung adenocarcinoma originated from epithelial cells, and their different cell origins do not rule out convergence at the level of intracellular signal pathways. In addition, the activation of PLCH MAPK pathway works together with inflammation and chemokine network to form lesions. At this time, postoperative tissue injury and subsequent repair, inflammatory signals related to fibrosis and immune remodeling induced by EGFR targeted therapy jointly form a microenvironment conducive to bone marrow cloning and amplification, namely MAPK mutation. This remodeling involves the changes of $CD8^+$ T cell infiltration, angiogenesis activity and the overall composition of immune cell population [21]. It is important that BRAF V600E acts as a constitutive active driver at RAF signal level, rather than through direct molecular crosstalk with EGFR. To sum up, sustained MAPK signal activation, postoperative lung tissue remodeling and immune microenvironment changes induced by EGFR targeted therapy may be the key mechanism factors of PLCH. According to the above observations, future research should focus on clarifying how the changes of pulmonary microenvironment after operation interact with mutations driven by MAPK pathway, so as to promote our understanding of the pathogenesis of PLCH, especially in non-smokers.

PLCH is composed of abnormal dendritic cells aggregated into loose tissues. These cells generally express CD1a and Langerin, which are distributed around the distal bronchioles and promote airway injury and parenchymal destruction [3, 25]. Immunohistochemical staining showed that the expression of CD1a and S-100 supported the identification of Langerhans cells. With the development of the disease, inflammatory cell infiltration will gradually turn into fibrosis, and cystic remodeling of lung parenchyma will also develop [2, 3]. In routine clinical practice, it is difficult to identify other lung diseases, especially in areas where tuberculosis is prevalent. In this case, CD1a, S-100 and langerin staining can provide some help for diagnosis and help to distinguish PLCH from infectious or granulomatous lesions. Therefore, the confirmation of histopathology is still very important when PLCH is suspected [26]. Therefore, in this case, the most direct evidence supporting PLCH instead of metastatic lung adenocarcinoma is the immunohistochemical results of biopsy specimens. The diseased cells were positive for CD1a, Langerin and S-100, but did not express markers related to lung adenocarcinoma, such as CK7, TTF-1 or Napsin A.

Patients with multiple system involvement or disease progression, who have received treatment before, generally need systematic treatment strategies. Commonly used treatment methods include methotrexate, low-dose cytarabine combined regimen (including cytarabine) and vinblastine combined with prednisone [27, 28]. It has been reported that cladribine (2-chlorodeoxyadenosine) can also improve the lung lesions of PLCH [29]. BRAF V600E mutation often appears in PLCH, which leads to the constitutive activation of MAPK signaling pathway and is considered as an important driving factor of disease progression [30]. Targeted therapies, including BRAF and MEK inhibitors, have shown clinical benefit in severe LCH, although relapse is common after discontinuation of MEK inhibitors [23, 31-33]. The BRAF V600E is a well-established oncogenic driver in melanoma, papillary thyroid carcinoma, and lung adenocarcinoma [34, 35]. However, to our knowledge, the concurrent presence of BRAF V600E mutations in both PLCH and lung adenocarcinoma has not been previously reported. A summary of the published literature was performed to identify ca-

Table 2. Cases on lung cancer and PLCH

Case Report	Age/ Gender	Smoke (pack-year)	Tumor Type	Tumor Stage	Genetic mutations in lung cancer/ PLCH	Postoperative Secondary/ Correlation (Remarks on Distinctive Features)	Outcomes/Treatment and PLCH response status
Kaya (2002) [39]	28/F	10	PAC	IIA	None	None/Coexistence	None/Surgery
Ohtsuki (2008) [12]	78/F	Never	PAC	IB	None	None/Coexistence	None/Surgery
Von der Thüsen (2011)	14/M	Never	PAC Thyroid carcinoma metastasis colonic carcinoma with MAP	IV	KRAS (p.G12C)/None	None/Coexistence	None/Chemotherapy
Bhardwaj (2013) [40]	28/F	10	PAC	IV	None	None/Coexistence	None/Chemotherapy
Kalchiem-Dekel (2017) [41]	56/F	55	PAC	IV	BRAF (p.V600E)/None	secondary PLCH	None/Chemotherapy+ Radiotherapy
Khaliq (2020) [42]	76/F	120	PAC	IIA	None	None/Coexistence	None/Surgery
Alden (2020) [43]	45/F	>30	PAC	IIIB	KRAS (p.G12D)/BRAF (p.V600E)	None/Coexistence	Alive/Neoadjuvant Chemotherapy+ Surgery
Gencer (2022) [1]	70/M	60	LSCC	IA	None/BRAF (p.V600E)	None/Coexistence	Alive/Surgery
Melocchi (2022) [44]	35/M	Yes	PAC	IIIB	KRAS (p.G12C)/BRAF (p.V600E)	None/Coexistence	Death (OS: 11 m)/Surgery
	72/M	Yes	PAC	IV	None/None	None/Coexistence	Death (OS: 8 m)/Surgery
	75/M	Yes	PAC	IB	KRAS (p.G13C)/None	None/Coexistence	Death (OS: 35 m)/Surgery
Sugihara (2024) [45]	74/F	27.5	PAC	IIA	None/None	Secondary PLCH	Alive/None
Our case	72/F	Never	PAC	IIIA	EGFR (p.L747_T751del)/BRAF (p.V600E)	Secondary PLCH (in situ)	Alive Icotinib, 125 mg TID (for multiple primary lung nodules) Significant reduction in PLCH

Abbreviations: PAC: pulmonary adenocarcinoma; LSCC: lung squamous cell carcinoma; MAP: MUTYH-associated polyposis; OS: overall survival.

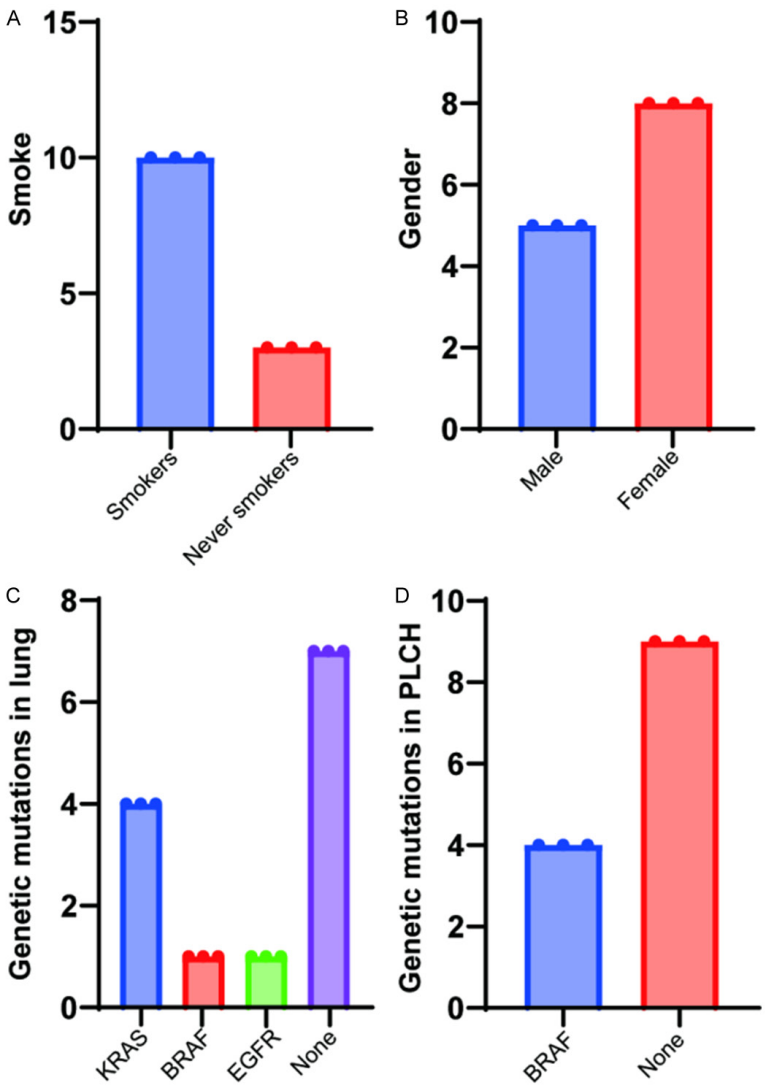

Figure 4. Pooled analysis of data from previously published reports. A. Number of patients with a history of smoking. B. Gender distribution. C. Genetic mutations identified in lung adenocarcinoma. D. Genetic mutations identified in PLCH.

ses of PLCH developing after lung adenocarcinoma resection or coexisting with lung cancer. The relevant data were extracted, compiled, and statistically analyzed (**Table 2** and **Figure 4**). It remains unclear whether BRAF V600E-mutated PLCH has the potential to progress toward lung adenocarcinoma or whether PLCH may promote adenocarcinoma development. Targeting BRAF V600E may therefore represent a therapeutic option relevant to both diseases. At present, no standardized treatment strategy exists for PLCH, and management is largely symptomatic. Pulmonary function may deteriorate over the first two years in a subset of patients. In contrast, improvement or disease stabilization has been observed in certain individuals receiving cladribine. Smoking cessation remains a key component of PLCH management, as isolated PLCH has been shown to improve markedly or even resolve following smoking cessation [2, 3, 36-38].

Conclusion

PLCH developing after surgical treatment for lung adenocarcinoma is seldom encountered. When new pulmonary lesions appear during postoperative follow-up, recurrence is often suspected; however, alternative diagnoses should also be considered. In this context, reliance on imaging findings alone may be insufficient. Imaging may be insufficient to establish a clear diagnosis of PLCH. Tissue examination provides essential pathological information, and molecular testing can be considered based on the clinical context.

Acknowledgements

This research was funded by the Tianjin Municipal Health Commission, the Tianjin Key Medical Discipline Sub-project (TJLCMS2021-06), the Tianjin Municipal Education Commission through the General Project of the Natural Science Foundation (2020KJ-162), the Wu Jieping Medical Foundation (320.6750.2022-11-43), the National Natural Science Foundation of China (8217-2569), the Natural Science Foundation of Tianjin (23JCYBJC01010), and the Tianjin Key Medical Discipline (Specialty) Construction Project (TJYXZDXK-061B). Additional support was provided by the Tianjin Key Medical Discipline Construction Funding Program (TJYXZDXK-3-002B and TJYXZDXK-3-006A-2), the Key R&D Program for International Science and

Technology Cooperation of the Gansu Provincial Science and Technology Program (23YFWA0005), the Innovation Fund for Colleges and Universities of Gansu Province (2025A-110), the Collaborative Innovation Center for Traditional Chinese Medicine Prevention and Control of Nutrition- and Environment-Related Diseases in Northwest China (ZYXT-24-02), the Natural Science Project of the Gansu Provincial Department of Science and Technology (22JRSRA582), and the Natural Science Project of the Gansu Provincial Department of Science and Technology (2023A-088).

Written informed consent was obtained from the participants for the publication of the details of their medical cases and any accompanying images.

Disclosure of conflict of interest

None.

Address correspondence to: Haoling Zhang, Department of Biomedical Sciences, Advanced Medical and Dental Institute, Universiti Sains Malaysia Kepala Batas 13200, Penang, Malaysia. E-mail: zhanghaolingedu@163.com; Jun Chen and Honglin Zhao, Department of Lung Cancer Surgery, Center of Thoracic Surgery, Tianjin Medical University General Hospital, Tianjin 300052, People's Republic of China. E-mail: huntercj2004@qq.com (JC); navyzhao@aliyun.com (HLZ)

References

[1] Gencer A, Ozcibik G, Karakas FG, Sarbay I, Batur S, Borekci S and Turna A. Two smoking-related lesions in the same pulmonary lobe of squamous cell carcinoma and pulmonary Langerhans cell histiocytosis: a case report. World J Clin Cases 2022; 10: 6722-6727.

[2] Vassallo R, Harari S and Tazi A. Current understanding and management of pulmonary Langerhans cell histiocytosis. Thorax 2017; 72: 937-945.

[3] Lorillon G and Tazi A. How I manage pulmonary Langerhans cell histiocytosis. Eur Respir Rev 2017; 26: 170070.

[4] Li HS, Liu CM, Zheng SF, Wu P, Xu HY, Hao XZ, Li JL, Xing PY, Duan JC, Wang ZJ, Zhong J, Tian LY, Cui YY, Fang Q, Lei SY, Wang SH, Luo YJ, Wang ZY, Wang J, He J, Sun N and Wang Y. RANKL/PD-1 dual blockade demonstrates survival benefit for patients with advanced lung adenocarcinoma harboring KRAS mutations. Cell Rep Med 2025; 6: 102235.

[5] Kang HR, Cho JY, Lee SH, Lee YJ, Park JS, Cho YJ, Yoon HI, Lee KW, Lee JH and Lee CT. Role of low-dose computerized tomography in lung cancer screening among never-smokers. J Thorac Oncol 2019; 14: 436-444.

[6] Kim BG and Um SW. A narrative review of the clinical approach to subsolid pulmonary nodules. Ann Transl Med 2023; 11: 217.

[7] Vassallo R, Jensen EA, Colby TV, Ryu JH, Douglas WW, Hartman TE and Limper AH. The overlap between respiratory bronchiolitis and desquamative interstitial pneumonia in pulmonary Langerhans cell histiocytosis: high-resolution CT, histologic, and functional correlations. Chest 2003; 124: 1199-1205.

[8] Harmon CM and Brown N. Langerhans cell histiocytosis: a clinicopathologic review and molecular pathogenetic update. Arch Pathol Lab Med 2015; 139: 1211-1214.

[9] Shi W, Hu Y, Lan J, Xiong J and Li Z. Impact of intestinal immunologic barrier dysfunction on perioperative complications. Perioperative Precision Medicine 2025; 54-70.

[10] Cheng B, Li C, Zhao Y, Li J, Xiong S, Liang H, Liu Z, Zeng W, Liang W and He J. The impact of postoperative EGFR-TKIs treatment on residual GGO lesions after resection for lung cancer. Signal Transduct Target Ther 2021; 6: 73.

[11] Sadoun D, Vaylet F, Valeyre D, Natali F, Georges R, Allard P and Battesti JP. Bronchogenic carcinoma in patients with pulmonary histiocytosis X. Chest 1992; 101: 1610-1613.

[12] Ohtsuki Y, Uomoto M, Hachisuka Y, Kato M, Iguchi M, Lee GH and Furihata M. A rare case of coexistence of pulmonary adenocarcinoma with Langerhans' cell histiocytosis. Med Mol Morphol 2008; 41: 175-178.

[13] Lee HW, Jin KN, Lee JK, Kim DK, Chung HS, Heo EY and Choi SH. Long-term follow-up of ground-glass nodules after 5 years of stability. J Thorac Oncol 2019; 14: 1370-1377.

[14] Mazzone PJ and Lam L. Evaluating the patient with a pulmonary nodule: a review. JAMA 2022; 327: 264-273.

[15] Kim YT. Management of ground-glass nodules: when and how to operate? Cancers (Basel) 2022; 14: 715.

[16] Baig H, Sonavane S, Makey I, Mallea J and Khoor A. Pulmonary langerhans cell histiocytosis presenting as a solitary pulmonary nodule on a lung cancer screening CT. Case Rep Pulmonol 2020; 2020: 8872111.

[17] Zhou Z, Wu J, Jiang J, Zhou M, Guo W and Hu Y. A review of multimodal medical image fusion developments in traditional, model-based and learning-based approaches. Perioperative Precision Medicine 2025; 152-167.

[18] Roden AC, Hu X, Kip S, Parrilla Castellar ER, Rumilla KM, Vrana JA, Vassallo R, Ryu JH and

Yi ES. BRAF V600E expression in Langerhans cell histiocytosis: clinical and immunohistochemical study on 25 pulmonary and 54 extrapulmonary cases. Am J Surg Pathol 2014; 38: 548-551.
[19] Abla O. Langerhans cell histiocytosis: promises and caveats of targeted therapies in high-risk and CNS disease. Hematology Am Soc Hematol Educ Program 2023; 2023: 386-395.
[20] Badalian-Very G, Vergilio JA, Degar BA, MacConaill LE, Brandner B, Calicchio ML, Kuo FC, Ligon AH, Stevenson KE, Kehoe SM, Garraway LA, Hahn WC, Meyerson M, Fleming MD and Rollins BJ. Recurrent BRAF mutations in langerhans cell histiocytosis. Blood 2010; 116: 1919-1923.
[21] Jia Y, Li X, Jiang T, Zhao S, Zhao C, Zhang L, Liu X, Shi J, Qiao M, Luo J, Liu S, Han R, Su C, Ren S and Zhou C. EGFR-targeted therapy alters the tumor microenvironment in EGFR-driven lung tumors: implications for combination therapies. Int J Cancer 2019; 145: 1432-1444.
[22] Du Y, Karatekin F, Wang WK, Hong W and Boopathy GTK. Cracking the EGFR code: cancer biology, resistance mechanisms, and future therapeutic frontiers. Pharmacol Rev 2025; 77: 100076.
[23] Jouenne F, Benattia A and Tazi A. Pulmonary langerhans cell histiocytosis - an update on pathogenesis and treatment. Curr Opin Pulm Med 2023; 29: 451-458.
[24] Lin A, Wei T, Meng H, Luo P and Zhang J. Role of the dynamic tumor microenvironment in controversies regarding immune checkpoint inhibitors for the treatment of non-small cell lung cancer (NSCLC) with EGFR mutations. Mol Cancer 2019; 18: 139.
[25] Suri HS, Yi ES, Nowakowski GS and Vassallo R. Pulmonary langerhans cell histiocytosis. Orphanet J Rare Dis 2012; 7: 16.
[26] Roden AC and Yi ES. Pulmonary langerhans cell histiocytosis: an update from the pathologists' perspective. Arch Pathol Lab Med 2016; 140: 230-240.
[27] Miao HL, Zhao AL, Duan MH, Zhou DB, Cao XX and Li J. Clinical presentation and prognostic analysis of adult patients with Langerhans cell histiocytosis with pulmonary involvement. BMC Cancer 2020; 20: 911.
[28] Duan MH, Han X, Li J, Zhang W, Zhu TN, Han B, Zhuang JL, Wang SJ, Cao XX, Cai HC, Chen M, Yang C and Zhou DB. Comparison of vindesine and prednisone and cyclophosphamide, etoposide, vindesine, and prednisone as first-line treatment for adult Langerhans cell histiocytosis: a single-center retrospective study. Leuk Res 2016; 42: 43-46.
[29] Lin H and Cao XX. Current state of targeted therapy in adult langerhans cell histiocytosis and erdheim-chester disease. Target Oncol 2024; 19: 691-703.
[30] Kobayashi M and Tojo A. The BRAF-V600E mutation in circulating cell-free DNA is a promising biomarker of high-risk adult langerhans cell histiocytosis. Blood 2014; 124: 2610-2611.
[31] Jouenne F, Benattia A and Tazi A. Mitogen-activating protein kinase pathway alterations in langerhans cell histiocytosis. Curr Opin Oncol 2021; 33: 101-109.
[32] Li J, Zhai Q, Zhang W, Chen Y, Wang C, Deng X, Zhang H, Lin Z and Zhu Y. The multifunctionality of the caspase family of proteases: a new perspective beyond cell death. Mol Aspects Med 2025; 106: 101411.
[33] Sandai D, Du Z, Zhang H and Sun Q. Regulatory mechanisms and emerging diagnostic and therapeutic opportunities of non-coding RNAs in tumorigenesis: a pan-cancer perspective. Crit Rev Clin Lab Sci 2025; 1-57.
[34] Heritier S, Helias-Rodzewicz Z, Lapillonne H, Terrones N, Garrigou S, Normand C, Barkaoui MA, Miron J, Plat G, Aladjidi N, Pagnier A, Deville A, Gillibert-Yvert M, Moshous D, Lefevre-Utile A, Lutun A, Paillard C, Thomas C, Jeziorski E, Nizard P, Taly V, Emile JF and Donadieu J. Circulating cell-free BRAF(V600E) as a biomarker in children with Langerhans cell histiocytosis. Br J Haematol 2017; 178: 457-467.
[35] Zhang HL, Zhao R, Wang D, Mohd Sapudin SN, Yahaya BH, Harun MSR, Zhang ZW, Song ZJ, Liu YT, Doblin S and Lu P. Candida albicans and colorectal cancer: a paradoxical role revealed through metabolite profiling and prognostic modeling. World J Clin Oncol 2025; 16: 104182.
[36] Bernstrand C, Cederlund K, Sandstedt B, Ahstrom L, Lundell M, Dahlquist G and Henter JI. Pulmonary abnormalities at long-term follow-up of patients with Langerhans cell histiocytosis. Med Pediatr Oncol 2001; 36: 459-468.
[37] Tazi A. Adult pulmonary Langerhans' cell histiocytosis. Eur Respir J 2006; 27: 1272-1285.
[38] Zhang H, Yan Q, Jiang S, Hu D, Lu P, Li S, Sandai D, Zhang H, Zhang W and Zhu C. Protein post-translational modifications and tumor immunity: a pan-cancer perspective. Phys Life Rev 2025; 55: 142-209.
[39] Kaya A, Savas Y, Sen E, Sak SD, Gungor A and Gonullu U. Histiocytosis X and bronchopulmonary adenocarcinoma: a rare coexistence. Can Respir J 2002; 9: 431-432.
[40] von der Thusen JH, van de Wetering MD, Westermann AM, Heideman DA and Thunnissen E. Bronchioloalveolar adenocarcinoma and pulmonary langerhans cell histiocytosis in a pa-

tient with MUTYH-associated polyposis. J Clin Oncol 2011; 29: e188-190.
[41] Kalchiem-Dekel O, Paulk A, Kligerman SJ, Burke AP, Shah NG and Dixon RK. Development of pulmonary Langerhans cell histiocytosis in a patient with established adenocarcinoma of the lung. J Thorac Dis 2017; 9: E1079-E1083.
[42] Khaliq MF, Noorani MM, Tariq SM, Koirala A and Mohamed H. Pulmonary langerhans cell histiocytosis associated with bronchogenic carcinoma. Cureus 2020; 12: e6634.
[43] Alden SL, Swanson SJ, Nishino M, Sholl LM and Awad MM. BRAF-mutant pulmonary langerhans cell histiocytosis mimicking recurrence of early-stage KRAS-mutant lung adenocarcinoma. JTO Clin Res Rep 2021; 2: 100127.
[44] Melocchi L, Mondoni M, Malapelle U and Rossi G. Langerhans cell histiocytosis-associated pulmonary adenocarcinoma: a word of caution during molecular determinations. Journal of Molecular Pathology 2022; 3: 286-292.
[45] Sugihara M, Okamoto S and Taniguchi T. Pulmonary Langerhans cell histiocytosis with multiple cavitary nodules after lung cancer surgery. Respirol Case Rep 2024; 12: e70028.

Supplementary Materials

ZYY-IRB-SOP-016(F)-002-03

Ethical Review Approval

Approval No.	IRB2024-YX-045-01		
Project Title	A retrospective study on the correlation among molecular classification, laboratory tests, imaging findings, treatment regimens, and prognosis of patients with pulmonary tumors		
Project Source	Self-initiated project		
Institution	Department of Pulmonary Oncology Surgery, Tianjin Medical University General Hospital		
Principal Investigator	Chen Jun		
Review Category	Initial Review	**Review Method**	Meeting Review
Review Date	February 28, 2024	**Review Venue**	Tianjin Medical University General Hospital, Second Conference Room, Third Inpatient Building
Review Committee Members	Zhang Zhikui, Fu Rong, Guo Fengxia, Jiang Rongcai, Hu Wen, Gu Jinxian, Zhu Mei, Lin Mei, Zhang Qingyu, Kang Chunsheng, Wan Chunxiao		
Approved Documents	Clinical Research Protocol (Version No.: 01; Version Date: 20240210) Statement on Waiver of Informed Consent		

Review Opinion:

According to the ethical principles set forth in the Measures for Ethical Review of Biomedical Research Involving Human Subjects (Trial, 2016), the NMPA Good Clinical Practice for Drug Clinical Trials (2020), the Good Clinical Practice for Medical Device Clinical Trials (2022), the WMA Declaration of Helsinki, and the CIOMS International Ethical Guidelines for Health-related Research Involving Humans, after review by this Ethics Committee, it is agreed that this study may be conducted in accordance with the approved research protocol, statement on waiver of informed consent, recruitment materials (if any), and subject-related materials (if any).

Please comply with the GCP principles, conduct the clinical study in accordance with the protocol approved by the Ethics Committee, and protect the health and rights of the subjects.

Before the study begins, the applicant shall complete clinical study registration.

During the study, if there is any change of principal investigator, or any amendment to the clinical research protocol, informed consent materials, recruitment materials, or other study documents, the applicant shall submit an amendment application for Ethics Committee review.

If a serious adverse event occurs, the applicant shall promptly submit a serious adverse event report. In accordance with the annual/periodic continuing review frequency specified by the Ethics Committee, the applicant shall submit a study progress report 1 month before the due date. The sponsor shall submit to the lead institution's Ethics Committee a summary report on the progress of the study at each center. If any circumstance arises that may significantly affect the conduct of the study or increase the risk to subjects, the applicant shall promptly submit a written report to the Ethics Committee.

If subjects not meeting inclusion criteria or meeting exclusion criteria are enrolled; if subjects who should be withdrawn according to the protocol are not withdrawn; if incorrect treatment or dose is given; if concomitant medication prohibited by the protocol is used; or if any other deviations from the approved protocol occur that may adversely affect subjects' rights, health, or the scientific validity of the study, the sponsor / monitor / investigator shall submit a protocol deviation report.

If the applicant suspends or terminates the clinical study early, please submit a study suspension / termination report in a timely manner.

Upon completion of the clinical study, please submit a study summary report.

Contact Person and Tel.	Jin Donglai 022-60363044
Signature of Chairperson	
Ethics Committee	Medical Ethics Committee of Tianjin Medical University General Hospital
Date	March 7, 2024

天津医科大学总医院 医学伦理委员会

Supplementary File 1

Workflow and procedures of NGS

For molecular analysis, formalin-fixed paraffin-embedded (FFPE) tissue specimens were sectioned at 4-5 μm thickness (approximately 10 sections per sample) for DNA extraction using a commercial tissue DNA extraction/purification kit. DNA quantity was assessed using the Qubit dsDNA HS Assay. For library preparation, 100 ng of DNA was mechanically fragmented to approximately 200 bp by ultrasonication, followed by end repair, adapter ligation, purification, and hybrid-capture enrichment. Libraries were quality-checked before sequencing, and paired-end 150-bp sequencing was performed on the DNBSEQ-T7 platform. Bioinformatic processing included demultiplexing, adapter trimming, quality filtering, alignment to the human reference genome (hg19), and variant calling for single nucleotide variants and small insertions/deletions. Copy number variation and structural variation analyses were also performed, followed by annotation using public and curated clinical databases. The quality-control thresholds were Q30 ≥80%, mean sequencing depth for tissue samples ≥500×, and target-region coverage ≥95%.

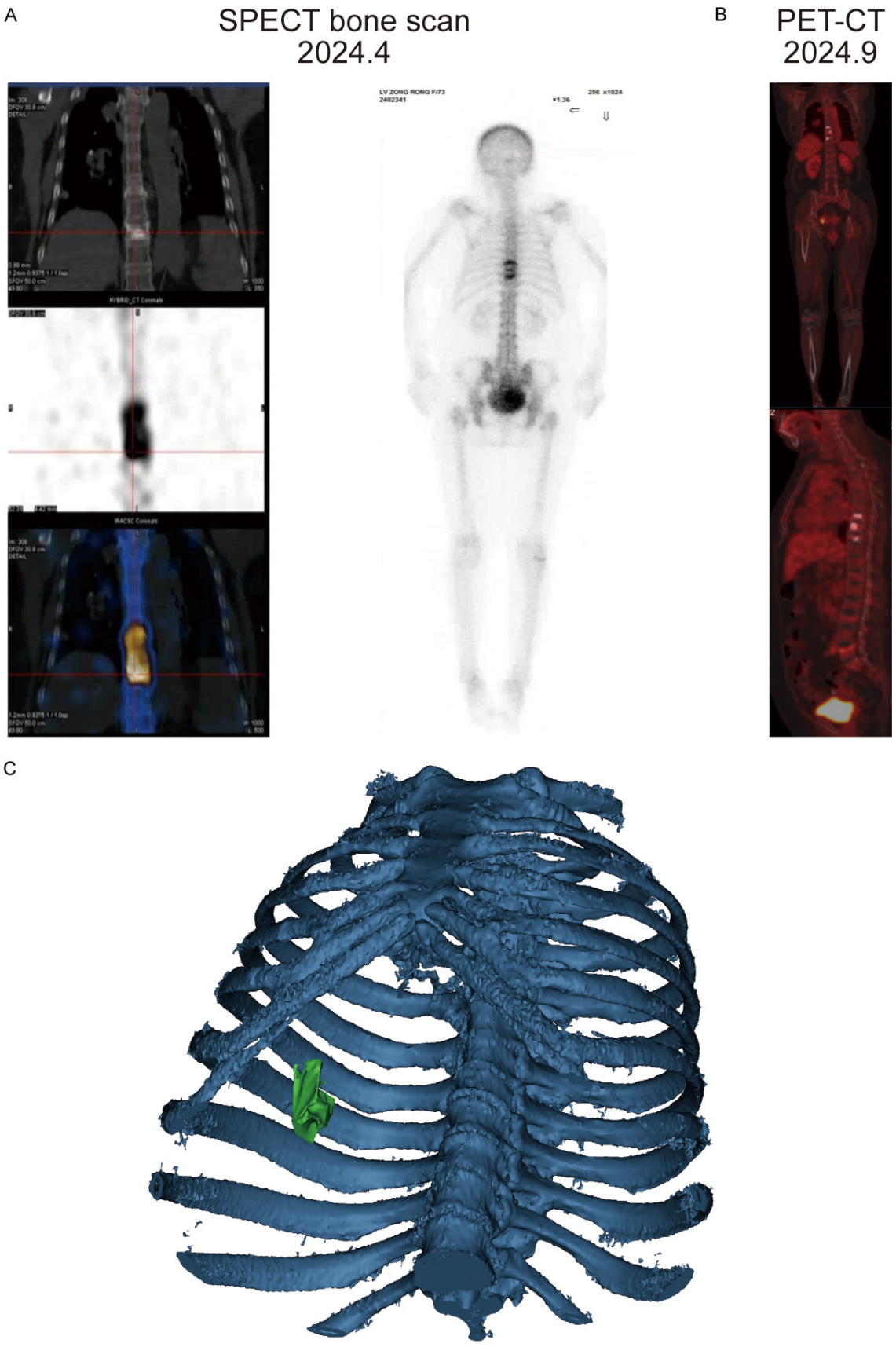

Supplementary Figure 1. Additional imaging reports. A. SPECT bone scan results. B. PET/CT findings. C. 3D reconstruction of PLCH and rib lesions.